



## D4.11.1: Report on the organization of test cases for aerosol typing method improvements



Deliverable no.	D4.11.1
Work package	WP4 – Atmosphere
Intermediate Objective	IO4.1
Deliverable type	<input checked="" type="checkbox"/> Document, report <input type="checkbox"/> Websites, patent filings, videos, etc. <input type="checkbox"/> Other: please specify .....
Dissemination level	<input checked="" type="checkbox"/> Public <input type="checkbox"/> Restricted
Estimated delivery (bimester)	B3
Actual delivery date	21.04.2023
Authors (Partner-OU)	Nikolaos Papagiannopoulos (CNR-IMAA)
Reviewed by	Lucia Mona (CNR-IMAA)
Comments	

## Index

<i>LIST OF TABLES AND FIGURES</i> .....	4
<i>1. INTRODUCTION</i> .....	5
<i>2. INSTRUMENTS</i> .....	5
<i>2.1 DISTRIBUTION OF AEROSOL LIDAR SYSTEMS</i> .....	7
<i>3. AEROSOL TYPING</i> .....	7
<i>3.1 AUTOMATIC TYPING METHODOLOGIES – A BRIEF DESCRIPTION</i> .....	7
<i>3.1.1 MAHALANOBIS DISTANCE TYPING ALGORITHM</i> .....	8
<i>3.1.2 NATALI (ARTIFICIAL NEURAL NETWORK) TYPING ALGORITHM</i> .....	9
<i>3.2 AUTOMATIC TYPING METHODOLOGIES – OTHER SOLUTIONS</i> .....	10
<i>3.2.1 TREE-LIKE AUTOMATIC AEROSOL TYPING</i> .....	10
<i>3.2.2 SCAN TYPING ALGORITHM</i> .....	11
<i>4. ORGANIZATION/RULES</i> .....	12
<i>4.1 METHODOLOGY GUIDELINES</i> .....	12
<i>4.2 DATA GUIDELINES</i> .....	13
<i>4.2 TEST CASES AND IMPLEMENTATION</i> .....	13
<i>REFERENCES</i> .....	15

## LIST OF TABLES AND FIGURES

<b>Table 1:</b> Italian lidar stations (1st column) according to their lidar setup, ACTRIS/EARLINET label, ACTRIS DB, and time span. The column ACTRIS DB holds info regarding whether data are uploaded in the database, if any. Time span refers to period the system is/has been active. ....	6
<b>Table 2:</b> The MD aerosol types for $3\beta+2\alpha+1\delta$ and $3\beta+2\alpha$ . $\kappa\beta$ is the backscatter-related Ångström exponent. ....	9
<b>Table 3:</b> The NATALI aerosol types for the 2 different modes. Colour ratio is the ratio of the particle backscatter coefficient of the longest wavelength over the backscatter coefficient of the shorter wavelength. ....	10
<b>Table 4:</b> The aerosol types considered for the tree-like automatic aerosol typing. ....	11
<b>Table 5:</b> The aerosol types considered for the SCAN algorithm. *Aerosol types, here, indicate the originating source of the air parcel assumed by Hysplit simulations. ....	11
<b>Table 6:</b> Overview of the automatic aerosol typing algorithms with the requirements (i.e., lidar setup), strengths, and limitations. <sup>1</sup> Papagiannopoulos et al. (2018). <sup>2</sup> Nicolae et al. (2018). <sup>3</sup> Baars et al. (2017). <sup>4</sup> Mylonaki et al. (2021). ....	12
<b>Figure 1:</b> ACTRIS/EARLINET stations – independently of the network label – grouped for lidar configuration, geographical distribution, and environment. ....	7
<b>Figure 2:</b> A generalized scheme for an automatic aerosol classification. The raw lidar data are converted to standard optical products and data quality control is checked. The layer-mean intensive properties are estimated and act as input for the aerosol typing. The selected typing methodology is tasked with the aerosol type assignment. ....	8

## 1. INTRODUCTION

This document sets the rules for this Activity (Act. 4.11) and aims, at first, to overview the instrumentation, infrastructure, and aerosol typing methodologies. Then, the document paves the way for the next steps to be followed and can act as Roadmap for this Activity. Aerosol typing is of particular interest for ITINERIS (WP4 – Atmosphere) since the knowledge of the aerosol types and sources can help to better understand the uncertain aspects of climate change projections.

Lidar systems can identify multiple layers in the atmosphere owing to their high vertical resolution. Thus, lidar-based retrievals can provide a separate classification for each layer and are not confined to columnar classifications as in the case of sun photometers. Therefore, lidar is a key instrument to infer aerosol types in complex aerosol scenes. The lidar technique has proven to be a robust tool to classify aerosols with its capability of polarization-sensitive and multi-wavelength measurements (e.g., Nicolae et al., 2018; Papagiannopoulos et al., 2018). Typically, the particle extinction-to-backscatter ratio (i.e., particle lidar ratio), the particle linear depolarization ratio at one or more wavelengths, and the wavelength dependence of extinction and/or backscatter coefficients (i.e., extinction- or backscatter-related Ångström exponents) are used. These intensive properties characterize different aerosol types and are independent of the aerosol load in the atmosphere. Even intensive properties might not be sufficient to guarantee accurate typing, as some aerosol types (e.g., biomass burning and industrial pollution) have very similar intensive properties but are attributed to different sources and generating mechanisms. It thus becomes clear that aerosol typing is a tedious and multiparametric task.

The deployment of new advanced lidars as well as unattended operation call for automatic typing procedures to tackle the ever-increasing amount of information and the inherent difficulty to separate aerosol types. Automatic algorithms are, therefore, employed to objectively classify aerosol into respective types. These procedures make use of the intensive properties that can quantify the differences between the aerosol classes and, ultimately, allocate the observed aerosol to a known aerosol type.

In the following, we focus on aerosol lidar instruments available in Italy and discuss the instruments, geographical distribution, and frequently encountered aerosol types over the Italian lidar stations. We briefly describe the available typing methods that were developed within the frame of ACTRIS/EARLINET and beyond, discussing the strengths and weaknesses. Finally, a tentative plan for the next steps with clear guidelines is presented.

## 2. INSTRUMENTS

EARLINET (<https://www.earlinet.org>) was established in 2000, providing aerosol profiling data on a continental scale, and is now part of the Aerosols, Clouds, and Trace gases Research InfraStructure (ACTRIS; <https://www.actris.eu/>). In these 23

years of continuous existence, EARLINET has evolved both in the number of contributing stations and in its observing capacity (Pappalardo et al., 2014). Currently, 31 stations are submitting aerosol extinction and/or backscatter coefficient profiles to the EARLINET database. EARLINET is not a federated network, and discrepancies are expected among the operating instruments (number of available channels, wavelengths, depolarization channel).

Typically, a  $3\beta+2\alpha+1\delta$  lidar configuration (i.e., 3 particle backscatter coefficient profiles, 2 particle extinction coefficient profiles, and 1 particle linear depolarization ratio profile) is opted for a comprehensive aerosol typing. The aerosol typing is based on intensive properties that are type sensitive. Three main intensive parameters are used to separate among the different aerosol types: particle depolarization ratio, Ångström exponent (or Colour index, or Colour ratio), and lidar ratio. Particle depolarization ratio is a shape indicator and an important quantity to separate among spherical and aspherical particles. Ångström exponent is size-dependent, and it is used to separate small-sized particles, e.g., pollution, from big-sized particles, e.g., marine aerosol. Whereas lidar ratio depends on the shape, size, and chemical composition of the aerosol.

In the frame of ACTRIS/EARLINET, the lidar stations can be labelled as active, joining, not permanent, and not active following the network's by-laws. Table 1 lists the Italian lidar stations according to their label (if part of ACTRIS/EARLINET) and lidar configuration that is important for the aerosol typing. Note that Ispra belongs to ACTRIS however is not part of ITINERIS. Additionally, the table lists whether the stations have data in the ACTRIS database and the time span of observations indicating the active years of the station. As a rule of thumb, the more intensive optical properties available the more accurate the aerosol typing can be.

**Table 1:** Italian lidar stations (1st column) according to their lidar setup, ACTRIS/EARLINET label, ACTRIS DB, and time span. The column ACTRIS DB holds info regarding whether data are uploaded in the database, if any. Time span refers to period the system is/has been active.

Lidar Station	Lidar setup	Label	ACTRIS DB	Time span
Catania	N/A	Not permanent	x	
Ispra	$3\beta+2\alpha+1\delta$	Active	x	2006-pres.
L'Aquila	$1\beta+1\alpha$	Not active	x	2000-pres.
Lamezia Terme	$1\beta+1\alpha+1\delta$	Not active	x	2015
Lampedusa	N/A	Joining	x	2013-pres.
Lecce	$3\beta+2\alpha$	Active	x	2000-pres.
Napoli	$3\beta+2\alpha$	Active	x	2000-pres.
Nicolosi	N/A	Not permanent	x	
Potenza	$3\beta+2\alpha+1\delta$	Active	x	2000-pres.
Roma-Tor-Vergata	$2\beta+2\alpha$	Active	x	2017-pres.
S. Pietro Capofiume	$2\beta+2\alpha+1\delta$			2022-pres.

## 2.1 DISTRIBUTION OF AEROSOL LIDAR SYSTEMS

The stations can be separated in clusters according to the lidar setup, the geographical distributions, and the environment. The figure below shows the Italian territory and the lidar stations are colour coded accordingly.

To assess the aerosol types only 2 stations are equipped with the required lidar configuration for high resolution typing, namely the  $3\beta+2\alpha+1\delta$ : Ispra and Potenza. Lecce and Naples operate a  $3\beta+2\alpha$  lidar system, which in turn can only yield a low-resolution typing. Roma-Tor-Vergata station operates a  $2\beta+2\alpha$  system and it is not compatible with any of the typing schemes. L'Aquila is not an active station and it only operated a UV Raman lidar with no depolarization measurement capability. A new system is planned for L'Aquila for the activities of the ACTRIS National Facility. Nicolosi and Catania are listed as not permanent members. Lampedusa is labelled as joining member. Furthermore, Bologna and Lamezia are also equipped with Raman lidars.

With respect to geographical distribution, the stations can be separated in 3 distinct categories: Central/South, North, and Insular. Finally, the lidar stations can be classified in not strict manner as Continental, Pollution, Marine, and Volcanic. Note that for the environment classification, dust is not considered even though it is an important aerosol type, but we assume that can be encountered for all the stations, of course, with different intensity.

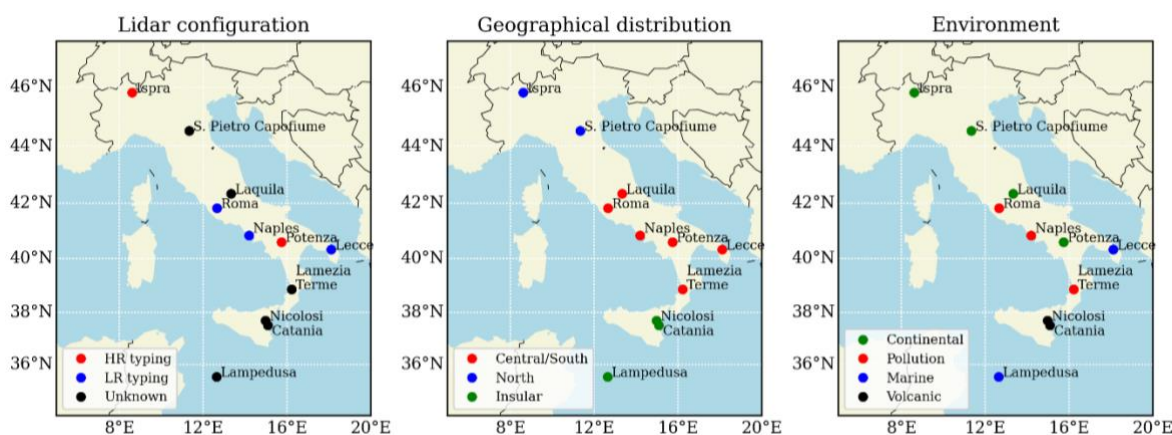


**Figure 1:** ACTRIS/EARLINET stations – independently of the network label – grouped for lidar configuration, geographical distribution, and environment.

## 3. AEROSOL TYPING

### 3.1 AUTOMATIC TYPING METHODOLOGIES – A BRIEF DESCRIPTION

The lidar technique has proven to be a robust tool to classify aerosols with its capability of polarization-sensitive and multi-wavelength measurements. Sophisticated lidars offer a multitude of intensive parameters that characterize

different aerosol types. The extensive aerosol parameters – aerosol backscatter coefficient, aerosol extinction coefficient, and aerosol optical depth – are not used since these parameters can vary with aerosol amount as well as type. Typically, the particle extinction-to-backscatter ratio (i.e., particle lidar ratio), the particle linear depolarization ratio at one or more wavelengths, and the wavelength dependence of extinction and/or backscatter coefficients (i.e., extinction- or backscatter-related Ångström exponents) are considered.

The layer-mean intensive properties are therefore input for the automatic aerosol typing schemes. Central to all typing procedures is the high-quality of the input data that can be ensured through consistent instrument calibration and data quality control. Differently, not quality assured data can lead to non-realistic results. ACTRIS/EARLINET, as a well-established network/infrastructure, offers quality-assured, widespread (continental-scale) observations.

Typically, the automatic typing classifies the layer-mean intensive properties by comparison with an aerosol model. The aerosol model is produced either by known samples of aerosol types or modelled aerosol types. The aerosol type assignment is the output of the typing methodology. The figure below illustrates the different steps of an automatic aerosol classification.

Within the framework of ACTRIS/EARLINET, two automatic aerosol typing schemes have been developed and can be the cornerstone of this activity. The SCC (Single Calculus Chain) tool for automatic processing of EARLINET lidar signals currently provides profiles of aerosol optical profiles (i.e., particle backscatter coefficient, particle extinction coefficient, and particle depolarization ratio). The SCC aims at incorporating modules for layer identification, intensive properties retrieval, and aerosol typing.

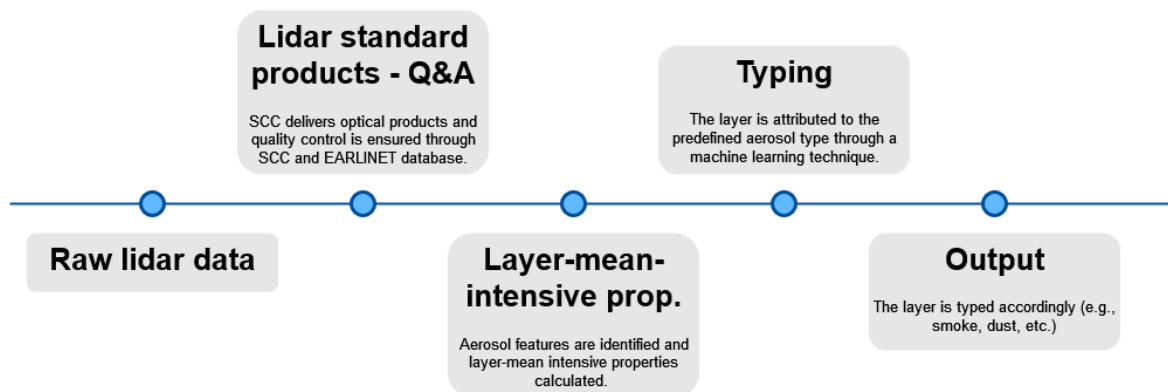


**Figure 2:** A generalized scheme for an automatic aerosol classification. The raw lidar data are converted to standard optical products and data quality control is checked. The layer-mean intensive properties are estimated and act as input for the aerosol typing. The selected typing methodology is tasked with the aerosol type assignment.

### 3.1.1 MAHALANOBIS DISTANCE TYPING ALGORITHM

The EARLINET Mahalanobis distance-based typing algorithm is a method specifically developed for the use on the EARLINET database with a high level of agility to accommodate the different lidar setups and needs (Papagiannopoulos et al.,

2018). The classification of each aerosol layer is made by calculating the distance of an observation from the predefined reference classes and by attributing each observation to a specific class based on the minimum distance. The reference dataset is solely made of EARLINET layer-mean-intensive optical parameters, and the classes comprise the typical aerosol components presented over Europe. The algorithm applies the Mahalanobis distance classifier to classify observations into a maximum of eight for a  $3\beta+2\alpha+1\delta$  lidar configuration. Table 2 lists the aerosol types and needed intensive properties for the maximum required lidar configuration and minimum required lidar configuration.

**Table 2:** The MD aerosol types for  $3\beta+2\alpha+1\delta$  and  $3\beta+2\alpha$ .  $\kappa_\beta$  is the backscatter-related Ångström exponent.

	<b>Lidar setup: <math>3\beta+2\alpha+1\delta</math></b>	<b>Lidar setup: <math>3\beta+2\alpha</math></b>
<b>Aerosol types</b>	<ul style="list-style-type: none"> <li>• Dust</li> <li>• Volcanic</li> <li>• Mixed Dust (Dust + Marine)</li> <li>• Polluted Dust (Dust + Smoke and/or Dust + Polluted Continental)</li> <li>• Clean Continental</li> <li>• Mixed Marine</li> <li>• Polluted Continental</li> <li>• Smoke</li> </ul>	<ul style="list-style-type: none"> <li>• Dust + Mixed Dust + Polluted Dust + Volcanic (dust-like aerosol types)</li> <li>• Clean continental</li> <li>• Mixed Marine</li> <li>• Polluted Continental + Smoke (small size with high lidar ratio values)</li> </ul>
<b>Intensive properties</b>	<ul style="list-style-type: none"> <li>• <math>\kappa_\beta(355-1064\text{ nm})</math></li> <li>• Lidar ratio at 532 nm</li> <li>• Ratio of the lidar ratios (532/355)</li> <li>• Depolarization ratio at 532 nm</li> </ul>	<ul style="list-style-type: none"> <li>• <math>\kappa_\beta(355-1064\text{ nm})</math></li> <li>• Lidar ratio at 532 nm</li> <li>• Ratio of the lidar ratios (532/355)</li> </ul>

### 3.1.2 NATALI (ARTIFICIAL NEURAL NETWORK) TYPING ALGORITHM

The NATALI (Neural network Aerosol Typing Algorithm based on Lidar data) software relies on artificial neural networks (Nicolae et al., 2018). It identifies the most probable aerosol type using a combination of layer-mean-intensive optical parameters (i.e., lidar ratios, Ångström exponent, colour ratios) from the provided aerosol backscatter and extinction coefficient profiles of lidar systems, without any additional information. The trained dataset consists of synthetic/modelled data. Depending on the availability of the particle linear depolarization ratio and the quality of the provided lidar profiles, the derived typing can be either of high resolution, or low resolution with depolarization, or low resolution without depolarization. Table 3 below lists the aerosol types considered for the 3 different modes of NATALI as well as the set of intensive properties.

**Table 3:** The NATALI aerosol types for the 2 different modes. Colour ratio is the ratio of the particle backscatter coefficient of the longest wavelength over the backscatter coefficient of the shorter wavelength.

	<b>Lidar setup: 3<math>\beta</math>+2<math>\alpha</math>+1<math>\delta</math> (high resolution)</b>	<b>Lidar setup 3<math>\beta</math>+2<math>\alpha</math>+1<math>\delta</math> (low resolution)</b>	<b>Lidar setup 3<math>\beta</math>+2<math>\alpha</math> (low resolution)</b>
<b>Aerosol types</b>	<ul style="list-style-type: none"> <li>• Continental</li> <li>• Continental Polluted</li> <li>• Dust</li> <li>• Maritime/Clean Continental</li> <li>• Smoke</li> <li>• Volcanic</li> <li>• Coastal</li> <li>• Coastal Polluted</li> <li>• Continental Dust</li> <li>• Continental Smoke</li> <li>• Dust Polluted</li> <li>• Maritime Mineral</li> <li>• Mixed Dust</li> <li>• Mixed Smoke</li> </ul>	<ul style="list-style-type: none"> <li>• Continental</li> <li>• Continental Polluted</li> <li>• Smoke</li> <li>• Dust</li> <li>• Maritime</li> <li>• Volcanic</li> </ul>	<ul style="list-style-type: none"> <li>• Dust</li> <li>• Continental Polluted</li> <li>• Smoke</li> <li>• Continental</li> <li>• Maritime</li> </ul>
<b>Intensive properties</b>	<ul style="list-style-type: none"> <li>• <math>\kappa_{\alpha}</math>(355-532 nm)</li> <li>• <math>\kappa_{\beta}</math>(532-1064 nm)</li> <li>• <math>\kappa_{\beta}</math>(355-532 nm)</li> <li>• Colour ratio 532/1064</li> <li>• Colour ratio 355/532</li> <li>• Lidar ratio 355</li> <li>• Lidar ratio 532</li> <li>• Depolarization ratio at 532</li> </ul>	<ul style="list-style-type: none"> <li>• <math>\kappa_{\alpha}</math>(355-532 nm)</li> <li>• <math>\kappa_{\beta}</math>(532-1064 nm)</li> <li>• <math>\kappa_{\beta}</math>(355-532 nm)</li> <li>• Colour ratio 532/1064</li> <li>• Colour ratio 355/532</li> <li>• Lidar ratio 355</li> <li>• Lidar ratio 532</li> <li>• Depolarization ratio at 532</li> </ul>	<ul style="list-style-type: none"> <li>• <math>\kappa_{\alpha}</math>(355-532 nm)</li> <li>• <math>\kappa_{\beta}</math>(532-1064 nm)</li> <li>• <math>\kappa_{\beta}</math>(355-532 nm)</li> <li>• Colour ratio 532/1064</li> <li>• Colour ratio 355/532</li> <li>• Lidar ratio 355</li> <li>• Lidar ratio 532</li> </ul>

## 3.2 AUTOMATIC TYPING METHODOLOGIES – OTHER SOLUTIONS

### 3.2.1 TREE-LIKE AUTOMATIC AEROSOL TYPING

A methodology based on thresholds obtained from multiyear, multisite EARLINET measurements for particle backscatter coefficient and particle depolarization ratio can derive four aerosol classes and many cloud classes (Baars et al., 2017). In particular, the particle backscatter at 532 nm and 1064 nm and particle depolarization ratio at 532 nm are used to classify aerosols by their physical features (shape and size). The technique uses a tree-like model of decisions similar to the aerosol classification of CALIPSO (Kim et al., 2018). The four aerosol types and the intensive properties are given in Table 4.

**Table 4:** The aerosol types considered for the tree-like automatic aerosol typing.

	<b>Lidar setup: <math>2\beta+1\delta</math> (532 nm and 1064 nm)</b>
<b>Aerosol types</b>	<ul style="list-style-type: none"> <li>• Aerosol: small</li> <li>• Aerosol: large, spherical</li> <li>• Aerosol: mixture, partly non-spherical</li> <li>• Aerosol: large, non-spherical</li> </ul>
<b>Intensive properties</b>	<ul style="list-style-type: none"> <li>• <math>\kappa_{\beta}</math>(532-1064 nm)</li> <li>• Depolarization ratio at 532 nm</li> </ul>

### 3.2.2 SCAN TYPING ALGORITHM

The Source Classification Analysis (SCAN; Mylonaki et al., 2021) tool is based on predefined and characterized aerosol source regions, the time that the air parcel spends above each geographical region, and a few additional criteria among which satellite products (e.g., GOME-2 NO<sub>2</sub> maps, MODIS FIRMS maps). It is a valuable tool to classify aerosol layers based on even single (elastic) lidar signals in the case of lidar stations that cannot provide a complete  $3\beta+2\alpha+1\delta$  dataset. Therefore, the only input are the time of the observation and the geometrical features of the aerosol layer from the lidar observations, and the typing assignment is based on Hysplit simulations. Note that the typing is made through a backward trajectory analysis and, thus, allocates aerosol layers to known sources and it is not based on type-dependent intensive properties. The tool can separate aerosol layers in six distinct aerosol types and it independent of lidar intensive properties (Tabl. 5).

Similarly, an interesting tool for height-resolved air mass source attribution has been developed and can complement lidar observations (Radenz et al., 2021). The tool uses dispersion model and geographical information and can be used independently of measurements.

**Table 5:** The aerosol types considered for the SCAN algorithm. \*Aerosol types, here, indicate the originating source of the air parcel assumed by Hysplit simulations.

	<b>Lidar setup: single wavelength</b>
<b>Aerosol types*</b>	<ul style="list-style-type: none"> <li>• Marine</li> <li>• Dust</li> <li>• Clean Continental</li> <li>• Continental Polluted</li> <li>• Smoke</li> </ul>
<b>Intensive properties</b>	<ul style="list-style-type: none"> <li>• Not needed</li> </ul>

In the next few months, a footprint analysis tool will be freely available within the H-2020 ATMO-ACCESS project with FLEXPART (FLEXible PARTicle dispersion model) simulations in different height levels. ITINERIS can profit from this development as it can assist in the assessment of the typing algorithms and also in the identification of the aerosol sources.

Table 6 summarizes the four described algorithms with their strengths and limitations. It also describes the required lidar setup.

**Table 6:** Overview of the automatic aerosol typing algorithms with the requirements (i.e., lidar setup), strengths, and limitations. <sup>1</sup>Papagiannopoulos et al. (2018). <sup>2</sup>Nicolae et al. (2018). <sup>3</sup>Baars et al. (2017). <sup>4</sup>Mylonaki et al. (2021).

Algorithm	Requirements	Strengths	Limitations
<b>MD<sup>1</sup></b>	<ul style="list-style-type: none"> <li>• Max lidar setup: <math>3\beta+2\alpha+1\delta</math></li> <li>• Min lidar setup: <math>2\beta+2\alpha</math></li> </ul>	<ul style="list-style-type: none"> <li>• Reference data adjustable</li> <li>• Class. param. adjustable</li> </ul>	<ul style="list-style-type: none"> <li>• No layering module</li> </ul>
<b>NATALI<sup>2</sup></b>	<ul style="list-style-type: none"> <li>• Max lidar setup: <math>3\beta+2\alpha+1\delta</math></li> <li>• Min lidar setup: <math>3\beta+2\alpha</math></li> </ul>	<ul style="list-style-type: none"> <li>• Highest number of aerosol classes</li> <li>• Layering module adapted</li> </ul>	<ul style="list-style-type: none"> <li>• Algorithm not adaptable</li> </ul>
<b>Tree-like typing<sup>3</sup></b>	<ul style="list-style-type: none"> <li>• Lidar setup: <math>2\beta+1\delta</math></li> </ul>	<ul style="list-style-type: none"> <li>• Easily adapted to a wide range of instruments</li> <li>• Simple approach</li> </ul>	<ul style="list-style-type: none"> <li>• No layering module</li> <li>• Built for calibrated high resolution lidar data.</li> <li>• Only four aerosol classes</li> </ul>
<b>SCAN<sup>4</sup></b>	<ul style="list-style-type: none"> <li>• Setup independent</li> </ul>	<ul style="list-style-type: none"> <li>• Applicable to every lidar configuration</li> </ul>	<ul style="list-style-type: none"> <li>• Dependent on model simulations</li> <li>• No layering module</li> <li>• Typing prone to error</li> <li>• High computational time</li> </ul>

## 4. ORGANIZATION/RULES

The organization of the Activity will be structured along the following lines. Note that modifications and/or deviations for some of the items below are expected.

### 4.1 METHODOLOGY GUIDELINES

1. The Activity is aiming to minimize effort and duplication by using existing tools (Section Aerosol typing) for a comprehensive aerosol typing. The main focus is on lidar setups equipped with  $3\beta+2\alpha+1\delta$  since 8 aerosol types or, ideally, more (MD: 8 types; NATALI: 14 types) are sufficient to describe the major aerosol components (Burton et al., 2012).

2. The input for the abovementioned methodologies is the required layer-mean-intensive properties (e.g., particle depolarization ratio). The intensive properties vary among the aerosol typing schemes, see Tables 2-5.

3. Modifications for MD and NATALI are not envisioned since training and testing are copious activities.

4. Considering the deployment of new advanced lidar systems, the benefit of the high space-time resolution aerosol typing will be showcased following the methodology of Baars et al. (2017). The ACTRIS/EARLINET SCC will soon implement a similar high resolution typing module.

5. Apart from the optical products, a typing module will be available at the ACTRIS Aerosol Remote Sensing Data Centre in synergy with this ITINERIS Activity.

## 4.2 DATA GUIDELINES

1. The quality of the lidar optical properties is of outmost importance for aerosol typing. Therefore, the Activity will make use of ACTRIS/EARLINET data where instrument calibration and quality-controlled data are ensured.

2. Furthermore, the ACTRIS/EARLINET SCC tool offers a layer product, which identifies the different aerosol layers in a single profile through a wavelet covariance technique and can be used to estimate the required layer-mean intensive properties. Note that NATALI incorporates a layering module based on detecting the strong gradient of the first derivative of the backscattered range-corrected lidar signal profile.

3. Data coming from instruments that are not compatible with the automatic aerosol typing schemes – i.e., NATALI and MD – or the data do not have a quality control track record but the lidar station presents an ideal test bed will be considered (e.g., Lampedusa). This can be achieved through the following steps:

- Data should follow the standard data and metadata of the respective RI (in this case ACTRIS/EARLINET).
- The flexible MD that can accommodate a  $2\beta+2\alpha$  lidar (wavelengths: 355 nm and 532 nm) and can distinguish 4 aerosol types.
- The tree-like typing that requires a  $2\beta+1\delta$  lidar system (backscatter coefficient wavelengths: 532 nm and 1064 nm; depolarization ratio wavelength: 532 nm) and can assign 4 aerosol types.
- The lidar setup-independent SCAN that is able to distinguish 6 aerosol types (i.e., originating sources).

## 4.2 TEST CASES AND IMPLEMENTATION

1. The plan is to use the historical data record of ACTRIS/EARLINET regardless of the label of the lidar station (e.g., not active, not permanent).

2. The focus is on specific sites with high scientific relevance: Lampedusa (dust, marine), Catania (volcanic emissions), Ispra (pollution).

3. For datasets outside the ACTRIS/EARLINET database, we will communicate with the data originator and seek for a possible solution engaging the ACTRIS/EARLINET SCC (Data #1 and Data #3).

4. Adaptation, if needed, of the existing algorithms will be considered (Data #3).

5. We will take profit of Intensive Observational Periods in the frame of ITINERIS. As an example, the planned IOP in Potenza in September where state-of-the-art lidars along with other remote sensing and in situ instruments will be present for the Activity 4.13. During this IOP, an ACTRIS/EARLINET intercomparison campaign will also take place. This opportunity will offer a data rich framework for algorithm testing and fine-tuning and, furthermore, can act as a bridge with other Activities/Objectives – e.g., Objective #3.
6. We will plan a campaign together with other Objectives/Actions to study specific aerosol types (e.g., dust, marine).
7. We will investigate possible synergies with other Objectives/Actions.

## REFERENCES

- Baars, H., Seifert, P., Engelmann, R., and Wandinger, U.: Target categorization of aerosol and clouds by continuous multiwavelength-polarization lidar measurements, *Atmos. Meas. Tech.*, 10, 3175–3201, <https://doi.org/10.5194/amt-10-3175-2017>, 2017.
- Burton, S. P., Ferrare, R. A., Hostetler, C. A., Hair, J. W., Rogers, R. R., Obland, M. D., Butler, C. F., Cook, A. L., Harper, D. B., and Froyd, K. D.: Aerosol classification using airborne High Spectral Resolution Lidar measurements – methodology and examples, *Atmos. Meas. Tech.*, 5, 73–98, <https://doi.org/10.5194/amt-5-73-2012>, 2012.
- Kim, M.-H., Omar, A. H., Tackett, J. L., Vaughan, M. A., Winker, D. M., Trepte, C. R., Hu, Y., Liu, Z., Poole, L. R., Pitts, M. C., Kar, J., and Magill, B. E.: The CALIPSO version 4 automated aerosol classification and lidar ratio selection algorithm, *Atmos. Meas. Tech.*, 11, 6107–6135, <https://doi.org/10.5194/amt-11-6107-2018>, 2018.
- Mylonaki, M., Giannakaki, E., Papayannis, A., Papanikolaou, C.-A., Komppula, M., Nicolae, D., Papagiannopoulos, N., Amodeo, A., Baars, H., and Soupiona, O.: Aerosol type classification analysis using EARLINET multiwavelength and depolarization lidar observations, *Atmos. Chem. Phys.*, 21, 2211–2227, <https://doi.org/10.5194/acp-21-2211-2021>, 2021.
- Nicolae, D., Vasilescu, J., Talianu, C., Biniotoglou, I., Nicolae, V., Andrei, S., and Antonescu, B.: A neural network aerosol-typing algorithm based on lidar data, *Atmos. Chem. Phys.*, 18, 14511–14537, <https://doi.org/10.5194/acp-18-14511-2018>, 2018.
- Papagiannopoulos, N., Mona, L., Amodeo, A., D’Amico, G., Gumà Claramunt, P., Pappalardo, G., Alados-Arboledas, L., Luís Guerrero-Rascado, J., Amiridis, V., Kokkalis, P., Apituley, A., Baars, H., Schwarz, A., Wandinger, U., Biniotoglou, I., Nicolae, D., Bortoli, D., Comerón, A., Rodríguez-Gómez, A., Sicard, M., Papayannis, A., and Wiegner, M.: An automatic observation based aerosol typing method for EARLINET, *Atmos. Chem. Phys.*, 18, 15879–15901, <https://doi.org/10.5194/acp-18-15879-2018>, 2018.
- Radenz, M., Seifert, P., Baars, H., Floutsi, A. A., Yin, Z., and Bühl, J.: Automated time–height-resolved air mass source attribution for profiling remote sensing applications, *Atmos. Chem. Phys.*, 21, 3015–3033, <https://doi.org/10.5194/acp-21-3015-2021>, 2021.